

# STRUCTURE AND MAGNETIC PROPERTIES OF NANOGRANULAR COMPOSITES CoFeZr-ALUMINA

A.M.Saad<sup>1</sup>, V.A. Kalaev<sup>2</sup>, J.A. Fedotova<sup>3</sup>, K.A. Sitnikov<sup>2</sup>, A.V. Sitnikov<sup>2</sup>,  
Yu.E. Kalinin<sup>2</sup>, A.K. Fedotov<sup>4</sup> and V.A. Svito<sup>4</sup>

<sup>1</sup> Al-Balqa Applied University, P.O.Box 2041, Amman 11953, Jordan

<sup>2</sup> Voronezh State Technical University, 394026 Voronezh, Russia

<sup>3</sup> National Centre for High Energy and Particle Physics of Belarusian State University, 153 M. Bogdanovich str., 220040 Minsk, Belarus

<sup>4</sup> Belarusian State University, Independence av. 4, 220050 Minsk, Belarus

Received: January 22, 2007

**Abstract.** The 5 to 15  $\mu\text{m}$  thick nanocomposite films  $(\text{Co}_{0.45}\text{Fe}_{0.45}\text{Zr}_{0.10})_x(\text{Al}_2\text{O}_3)_{1-x}$  with  $30 < x < 65$  at.% sputtered in a chamber evacuated with pure Ar gas were studied using Mössbauer spectroscopy, magnetization, complex magnetic permeability, and magneto-force microscopy (MFM) measurements. In particular, the films with  $x < 40$  at.% displayed superparamagnetic state at room temperature (the lack of sextets in Mössbauer spectra, non-hysteresis character of the magnetization curves, invariability of real  $\mu'$  and imaginary  $\mu''$  parts of magnetic permeabilities with  $x$  and high resistivity. Near the percolation threshold ( $x \approx 40 - 45$  at.%) Mössbauer spectra displayed features of the ferromagnetic sextet and the values of  $\mu'$  and  $\mu''$  increased, approaching the maximum, as  $x$  increasing due to the decrease of inter-particle distances. Moreover, effects of dipole-dipole and exchange interactions of the nanoparticles resulted in the nucleation of the magneto-ordered granules (magnetoclusters) including a few metallic nanoparticles. The MFM allowed to visualizing the presence of magnetic labyrinth-like magnetic contrast that was formed by the metallic nanoparticles near the percolation threshold. At  $x > 45$  at.% the films behave like the "bulk" ferromagnetic sample with occasional inclusions of dielectric phase.

## 1. INTRODUCTION

At present time high interest is given to granular composite materials, which consist of metallic nanosized particles randomly distributed within a dielectric matrix, because they represent nearly ideal systems for the study of nanostructured materials with a big change of their composition. For the first time, such materials (named as cermets) were manufactured at the beginning of seventies of the last century and during that decade the main concepts concerning the electrical and magnetic

properties of composites were stated [1-5]. The interest of these materials was renewed in the nineties, of the previous century, because of their possible applications in the magnetic field sensors and as magnetic recording media. The study of magnetic properties of iron, cobalt or nickel nanoparticles embedded into a dielectric matrix has shown [6] that reduction of volume fraction of the metallic phase below the percolation threshold  $x_c$  resulted in metallic granules becoming a single-domain and the nanocomposite as a whole displays superparamagnetic properties at room tem-

---

Corresponding author: A.K. Fedotov, e-mil: fedotov@bsu.by; AlexanderFedotov@newmail.ru

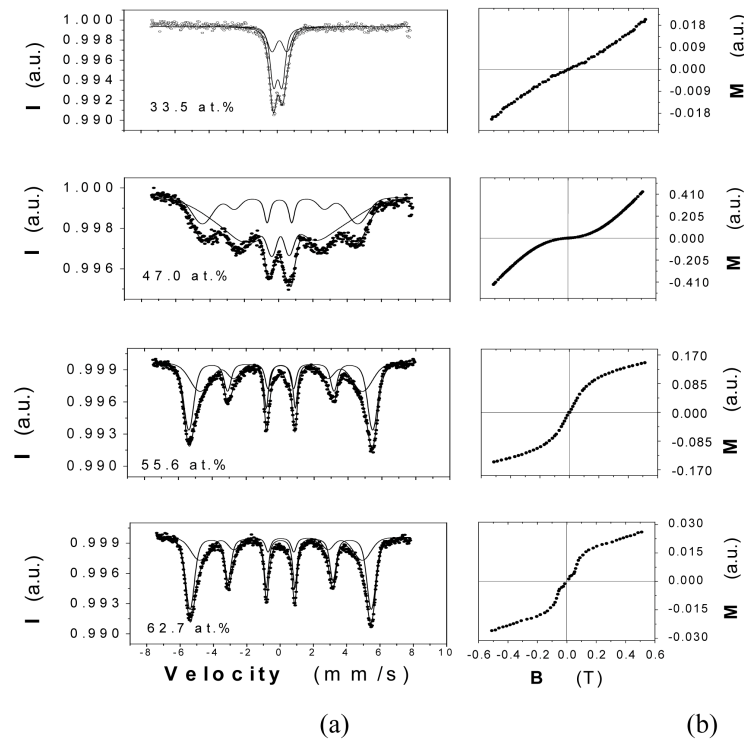


**Fig. 1.** Mössbauer spectra (a) and magnetization curves  $M(B)$  (b) for the as-deposited nanocomposite films.

perature. However, if volume ratio of the metal exceeds  $x_c$  such nanoparticles create a fractal net in the insulating matrix and the composites exhibit soft magnetic properties and demonstrate extraordinary electron transport behavior. For example, the composites consisting of iron, cobalt or nickel ferromagnetic single-domain nanoparticles embedded in metallic, semiconducting or insulating matrixes demonstrate giant and/or tunneling magnetoresistance [7-9] (approaching the values of 8% at room temperature [10]), anomalous Hall effect [11,12], high values of magnetorefractive, and Kerr effects [13-15], *etc.* The nanocomposites with insulating matrix are also quite promising for high frequency applications. Large value of permeability was demonstrated for thin films composite with cobalt nanoparticles at frequency  $\leq 1$  GHz [16-18].

Goal of the present paper is to investigate the influence of composition of the composite films, containing amorphous CoFeZr nanoparticles embedded into amorphous aluminium oxide matrix, on their phase composition, magnetic structure and the high-frequency complex magnetic permeability.

## 2. EXPERIMENTAL

The ferromagnetic alloy  $\text{Co}_{0.45}\text{Fe}_{0.45}\text{Zr}_{0.10}$  which has low coercivity is being used as a material for the formation of metallic nanoparticles in the studied composites. The composite films  $(\text{Co}_{0.45}\text{Fe}_{0.45}\text{Zr}_{0.10})_x(\text{Al}_2\text{O}_3)_{1-x}$  were prepared by ion-beam sputtering in a chamber contained low pressure pure Ar gas using compound target which consisted of alloy base with dimensions of  $280 \times 80$  mm<sup>2</sup> with some alumina plates arranged on its surface [19]. Irregular distribution of alumina plates at the target surface allowed this work getting a wide value of metal-to-dielectric ratio  $x$  (depending on the mutual arrangement of the target and substrates) in one technological cycle. Owing to the specific design of the vacuum set-up, sputtering of the target was carried out at low enough pressure ( $6.9 \cdot 10^{-2}$  Pa) that assured purity of the deposited film and extremely low content of Ar in the samples. The studied samples (films) were sputtered onto glass-ceramic substrates (for electric and magnetic measurements) and thin aluminum foils (for Mössbauer investigation) at the temperature  $\approx 373$ K. Thicknesses of the composite films were 5  $\mu\text{m}$  to 15  $\mu\text{m}$  and dimensions of the studied

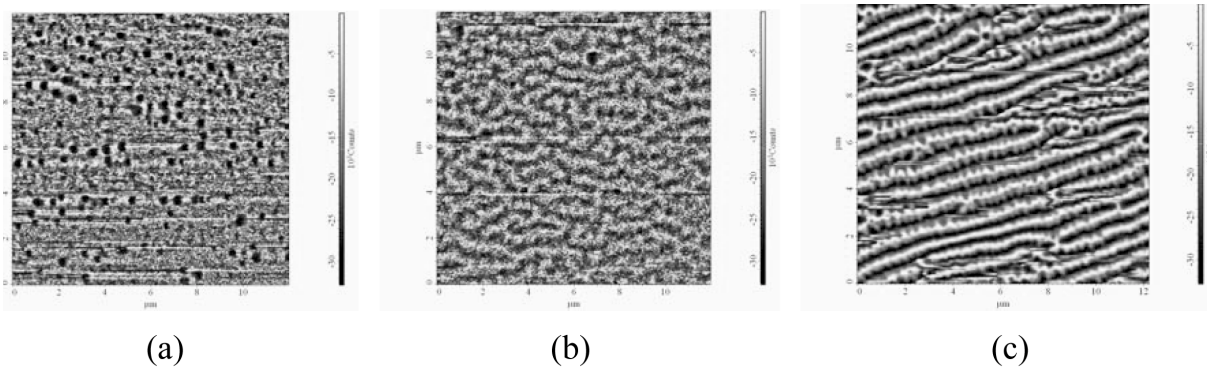


**Fig. 3.** MFM pictures showing magnetic contrast for the nanocomposites samples of metallic phase concentrations  $x$  of 33.3 at.% (a), 45.0 at.% (b), and 63.5 at.% (c).

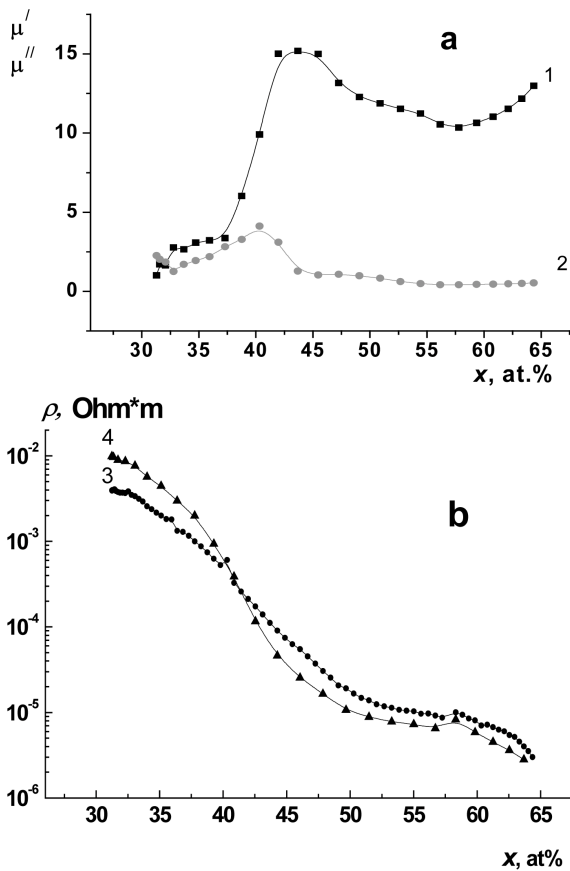


**Fig. 2.** Dependences of real  $\mu'$  (curve 1) and imaginary  $\mu''$  (curve 2) parts of complex permeability for  $f = 25$  MHz (a) and DC resistivities  $r$  (b) for the as-deposited (curve 3) and annealed in vacuum at 673K for 30 min (curve 4) nanocomposites versus metallic to dielectric phase ratio  $x$ .

samples together with the substrate were 60 mm long, 1.95 mm wide and 0.6 mm thick. Measurements of the chemical elements content of the composites were made using a special micro-probe X-

Ray analyses in LEO 1455VP with an accuracy of  $\sim 1\%$ . Structural characterization (phase composition and also the valence state of Fe ions) and magnetic state of the nanocomposites were made using Mössbauer spectroscopy. Mössbauer spectra were recorded in transmission geometry at room temperature using spectrometer MS2000 with  $^{57}\text{Fe}/\text{Rh}$  source and  $\text{YAlO}_3:\text{Ce}$  crystalline scintillation detector [20]. Magnetic permeability was measured by the resonance method [21] at the frequencies of 25 - 200 MHz with the orientation of the alternating measuring field  $B$  in the plane of the film and parallel to the sample axis. The ratio error for the real  $\mu'$  and imaginary  $\mu''$  parts of the permeability measurements was about 8%. Measurement of the magneto-response was made using the alternation grads magnetometer at 300K and 1 MHz with applied magnetic fields of  $B \leq 600$  mT (magnetization curves) and SolverPro atomic force microscope (the distribution of magnetic contrast) working in AC MFM regime, with a tip of cantilever covered with a CoCr 40 nm thickness layer. All experiments were carried out at room temperature.

### 3. RESULTS AND DISCUSSION

Mössbauer spectra and magnetization curves were measured with  $B$  normal to the film surface plane for the samples of atomic fraction ( $x$ ) of the nanoparticles alloy = 33% ÷ 64% are presented in Fig. 1. Interpretation of these data will be presented together with the discussion of high-frequency complex magnetic permeability  $\mu$  and MFM measurements below in Figs. 2 - 4. Fig. 2a shows that for the initial (as-deposited) samples, where metallic phase contents  $x$  in the range of 33 to 37 at.%, the values of real  $\mu'$  and imaginary  $\mu''$  parts of the complex permeability (curves 1 and 2 respectively) changed insignificantly due to superparamagnetic state of the films. The latter was also confirmed by

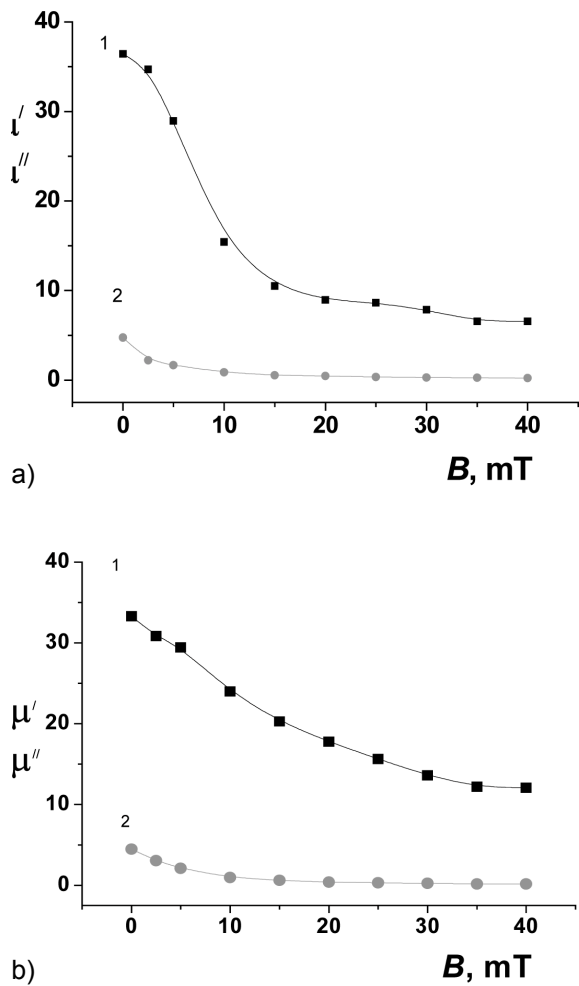


**Fig. 4.** Dependences of real  $\mu'$  (curve 1) and imaginary  $\mu''$  (curve 2) parts of the complex permeability measured at  $f = 16$  MHz for the as-deposited  $(\text{Co}_{0.45}\text{Fe}_{0.45}\text{Zr}_{0.10})_{0.42}(\text{Al}_2\text{O}_3)_{0.58}$  nanocomposite films versus magnetic field induction  $B$  directed along (a) and normal (b) to the sample axis.

the character of Mössbauer spectra (no sextet in Fig. 1a for  $x \approx 33$  at.%), the lack of hysteresis on magnetization curves (see Fig. 1b for  $x \approx 33$  at.%) and also high values of DC resistivities (see Fig. 2b for  $x < 37$  at.%).

Further rise of  $x$  beyond 37 at.% resulted in a strong increase of  $\mu'$  and also a quick decrease of  $\rho$  for the as-deposited films as shown in Fig. 2. These effects and the appearance of sextet com-

ponent in Mössbauer spectra (Fig. 1a) are evidence to demonstrate magnetic dipole-dipole interaction and the exchange interaction between the nanoparticles due to the decrease of the distances between them. This nucleation of the magneto-ordered state in the samples at  $x \sim 37$  at.% is probably coincided with the beginning of agglomeration of the nanoparticles into large-scale granules, i.e. formation of the so-called ferromagnetic clusters, which contain a few nanoparticles. The last is accompanied by the increase of magnetization with  $x$  [22]. Moreover, by approaching the percolation threshold  $x_c$ , the number and sizes of these ferromagnetic clusters in the dielectric matrix are growing and an infinite magnetic cluster can be formed close to the maximum of  $\mu'$  at  $x \approx 40$  at.%. Besides, just beyond this value of  $x$  a full transformation of Mössbauer spectra from doublet-like into sextet-like shape was observed (see Fig. 1a) confirming transition of the nanocomposite into ferromagnetic state.

As  $x$  increased to 40-45 at.% (curve 1 in Fig. 2a)  $\mu'$  increased to its maximum probably due to the formation of the labyrinth-like structure of ferromagnetic granules with preferred direction of magnetic moments in the dielectric matrix (see Fig. 3b). Note that replacement of alumina on silica in CoFeZr-based nanocomposites resulted in a big increase of  $\mu'$  and  $\mu''$  values [18] probably due to reduction of the interaction between ferromagnetic atoms as a result of dilution of nonferromagnetic Al atoms in the  $\text{Co}_{0.45}\text{Fe}_{0.45}\text{Zr}_{0.1}$  nanoparticles.

Further, at the magnetic phase concentration  $x > 45$  at.% the composite behaved like the "bulk" ferromagnetic sample with occasional inclusions of the dielectric phase and that resulted in the reduction of  $\mu'$  and  $\mu''$  at high frequencies (Fig. 2). This decrease of  $\mu'$  and  $\mu''$  just beyond the percolation threshold could be due to the formation of the so-called infinite magnetic cluster composed of electrically connected nanoparticles and that probably resulted in non-single-domain structure (see Fig. 1b for  $x \approx 62$  at.% and Fig. 3c). This also probably follows from the decrease of the integral magnetic moment just beyond the percolation threshold observed in [22].

Note that the percolation thresholds identified by different methods have essential distinctions. So the value of  $x_c \approx 40$  at.% fixed by the position of maxima on concentration dependences of magnetic permeability is a little less than the  $x_c \approx 41$  at.% determined from the intersection of the curves 1 and 2 in Fig. 2b for room-temperature resistivities

measured in as-deposited and annealed for 30 min at 673K samples respectively. At the same time, these both values of  $x_c$  are much less than that of  $x_c \approx 45 - 47$  at.% defined earlier by our work from magnetoresistance, magnetization, Mössbauer and impedance measurements [20,21]. These differences are probably due to the infinite magnetic cluster, contained some magnetic interacting granules, which is formed at slightly less values of  $x$  than the infinite current-conducting (percolating) cluster is formed from the electrically connected metallic nanoparticles. This assumption seems to be confirmed by the results of MFM measurements presented in Fig. 3.

In order to state the preferred direction of magnetization vectors in the ferromagnetic phase the complex magnetic permeability of the nanocomposites was studied depending on external magnetic field  $B$  and its orientation relative to the longitudinal axis of the samples. Fig. 4 shows the variation of real parts of the complex permeability  $\mu'(B)$  versus the external magnetic field  $B$  (along the sample axis) for the sample of  $x = 42$  at.%. When the orientation of the sample axis parallel to the probing high frequency magnetic field ( $B_{\parallel}$ ) and normal to the external magnetic field ( $B$ ) the variations of  $\mu'$  (Fig. 4b, curve 1) and  $\mu''$  (Fig. 4b, curve 2) versus  $B$  are smoothly receded.

Thus the conducted analysis of the presented results show that values of the complex magnetic permeability depend on both of the metal-to-dielectric fraction ratio and magnetic structure formed during preparation of the composite. Generally, the measured values of high-frequency  $\mu'$  and  $\mu''$  depend on two main factors: shift of domain boundaries and rotation of magnetization vector. Following the high frequency measurements, contribution from the domain wall shift to the complex magnetic permeability is negligible. Therefore, the change in permeability under the subject of external magnetic field is almost determined by the processes of rotation of the magnetization vector. In so doing, the above mentioned small inflection of curve  $\mu'(B)$  in Fig. 4a, when the orientations of  $B_{\parallel}$  and  $B$  are at the plane of the sample and along its longitudinal axis, is an evidence of mismatches between the preferred direction of light magnetization axis and the longitudinal axis of the sample that is also confirmed by MFM scanning data (Fig. 3).

As has been shown above, the values of the complex magnetic permeability of the composites are strongly dependent on their chemical compo-

sition and concentration of the metallic phase. In this connection, it is wise to underline two main features: Firstly, at room temperatures the low- $x$  composites display low values of complex magnetic permeability, high values of DC resistivities, the lack of hysteresis on magnetization curves and sextet component in the Mössbauer spectra indicating their superparamagnetic state. Secondly, for the studied nanocomposites the noticeable increase of high-frequency  $\mu'$  and  $\mu''$  with the increase of metallic phase concentration was observed early before the percolation threshold determined from the electric and Mössbauer measurements. This indicated that the magnetic interaction between the ferromagnetic nanoparticles occurred earlier than that when the nanoparticles joined electrically forming continuous percolating (current-conducting) cluster. Hence, the high-frequency technique measurement of the complex magnetic permeability can be used as a very sensitive method to indicate the initial stages of interaction of the ferromagnetic nanoparticles as the metallic phase concentration increases. For the studied composites this method in particular turned out to be sensitive indicator for the nucleation of the individual ferromagnetic granules, created by closely-situated nanoparticles but not connected electrically with each other, that increase in size as concentration of the metallic phase increases to 40 - 45 at.%. This transfers bulk of the composite into a magneto-ordered state accompanied by a further increase of the real part of the complex magnetic permeability approaching maximum of  $\mu(x)$  curve or inflection of  $\mu(B)$  curve near the percolation threshold  $x_c$  identified by the electrical measurements and Mössbauer spectra. Note that this transition into magneto-ordered state is also dependent on chemical composition of the nanoparticles and matrix, measurement method and frequency of the probing magnetic field.

The fact that the character of  $\mu(x)$  curves in the concentration region, when the magnetic ordering is nucleated, is strongly varied for different composites is probably an evidence of the essential inhomogeneity in the distribution of magnetic moments in the composite bulk, i.e. presence and type of the magnetic anisotropy which depends on the film composition and the conditions of their preparation. In the general case, the value of the complex magnetic permeability is firstly determined by the energy of magnetic anisotropy (crystalline, magnetoelastic, induced). Inasmuch as crystalline anisotropy for the studied nanocomposites is lacking, the main influence on the formation of their magnetic structure is determined by magnetoelastic

energy and the shape anisotropy ( $W_{SA}$ ) which is given by:

$$W_{SA} = -1/2H_0J,$$

where  $J$  is a microscopic magnetization of the material and  $H_0$  is the demagnetizing field. Note also that the composites which are beyond the percolation threshold and possess the fully ordered magnetic structure can be separated with respect to their magnetic state into two groups: (i) with labyrinth-like magnetic structure containing ferromagnetic current-conducting channels in the dielectric matrix (for  $x \leq 45$  at.%) and (ii) the "bulk" ferromagnetic state with the occasional inclusions of dielectric phase (for  $x > 45$  at.%).

#### 4. CONCLUSION

Analysis of the presented results shows that values of the complex magnetic permeability depend on both of the metal-to-dielectric fraction ratio and magnetic structure formed during the composite preparation. The composites before percolation threshold display at room temperature low values of the complex magnetic permeability, high values of DC resistivities, lack of hysteresis for the magnetization curves and sextet component in Mössbauer spectra indicating the superparamagnetic state. The noticeable increase of high-frequency  $\mu'$  and  $\mu''$  with the increase of metallic phase concentration, which observed before the percolation threshold determined from the electric and Mössbauer measurements, indicated that magnetic interaction between the ferromagnetic nanoparticles started before the nanoparticles joined into continuous percolating (current-conducting) cluster due to their electrical contacting. This transition towards the magneto-ordered state at  $x < x_c$  was accompanied by the formation of labyrinth-like magnetic structure in the nanocomposites confirmed by MFM measurements.

#### ACKNOWLEDGEMENT

The authors would like to acknowledge financial support from VISBY Program of the Swedish Institute, Belarusian Republican Fundamental Research Foundation by Contract F06P-128, Russian Foundation for Basic Research under Grant № 06-02-81035 and CRDF Grant N 05-010-1.

#### REFERENCES

[1] C.A. Neugebauer // *Thin Solid Films* **6** (1970) 443.

- [2] J.L. Gittleman, Y. Goldstain and S. Bozowski // *Physical Review B* **5** (1972) 3609.
- [3] B. Abeles, P. Sheng, M.D. Coutts and Y. Arie // *Adv. Physics* **24** (1975) 407.
- [4] A.L. Efros and B.I. Shklovski // *Uspehi Fizicheskikh Nauk* **117** (1974) 2, In Russian.
- [5] A.L. Efros and B.I. Shklovski // *Phys. Stat. Solidi A* **78** (1976) 475.
- [6] C.L. Chien // *Annu. Rev. Mater. Sci* **25** (1995) 129.
- [7] A. Gerber, A. Milner, B. Groisman and A. Gladkikh // *Phys. Rev. B.* **55** (1997) 6446.
- [8] S. Honda, T. Okada and M. Nawate // *J. Magn. Magn. Mater.* **165** (1997) 153.
- [9] K. Yakushiji, S. Mitani, K. Takanashi, J. -G. Ha and H. Fujimori // *J. Magn. Magn. Mater.* **212** (2000) 75.
- [10] H. Fujimori, S. Mitani and S. Ohnuma // *Mater. Sci. Eng. B* **31** (1995) 219.
- [11] B.A. Aronzon, A.E. Varfolomeev, A.A. Likalter, V.V. Rylkov and M.V. Sedova // *Fizika Tverdogo Tela (Soviet Solid State Physics)* **41** (1999) 944.
- [12] J.C. Denardin, A.B. Pakhomov, M. Knobel, H. Liu and X.X. Zhang // *J. Phys.: Cond. Matter* **12** (2000) 3397.
- [13] I.V. Bykov, E.A. Ganshina, A.B. Grnovski and V.S. Gushchin // *Fizika Tverdogo Tela (Russian Solid State Physics)* **42** (2000) 487.
- [14] A.V. Kimel, R.V. Pisarev, Yu.E. Kalinin, A.V. Sitnikov, O.V. Stogney, F. Bentivegna and Th. Rasing // *Fizika Tverdogo Tela (Russian Solid State Physics)* **45** (2003) 269.
- [15] I.V. Zolotukhin, Yu.E. Kalinin, P.V. Neretin, A.V. Sitnikov and O.V. Stogney // *Alternative Power and Ecology* **2** (2002) 7, In Russian.
- [16] S. Ohnuma, H. Fujimori, S. Mitani and T. Masumoto // *J. Appl. Phys.* **79** (1996) 5130.
- [17] Y. Hayakawa, A. Makino, H. Fujimori and A. Inoue // *J. Appl. Phys.* **81** (1997) 3747.
- [18] S. Ohnuma, H.J. Lee, N. Kobayashi, H. Fujimori and T. Masumoto // *IEEE Trans. Magn.* **37** (2001) 2251.
- [19] A.V. Sitnikov, In: *Proc. of Intern. Seminar on the Problems of Magnetism in Magnetic Films, Small Particles and Nanostructures* (Astrakhan, Russia, 2003), p. 75.
- [20] A.M. Saad, A.V. Mazanik, Yu.E. Kalinin, J.A. Fedotova, A.K. Fedotov, S. Wrotek, A.V. Sitnikov and I.A. Svito // *Rev. Adv. Mater. Sci.* **8** (2004) 34.

- [21] V.A. Kalaev, Yu.E. Kalinin, V.N. Necaev and A.V. Sitnikov // *Bulletin of Voronezh State Technical University: Material Science* **1.13** (2003) 38, In Russian.
- [22] A.M. Saad, A.K. Fedotov, J.A. Fedotova, I.A. Svito, B.V. Andrievsky, Yu.E. Kalinin, V.V. Fedotova, V. Malyutina-Bronskaya, A.A. Patryn, R.V. Mazanik and A.V. Sitnikov // *Phys. Stat. Sol. (c)* **3** (2006) 1283.
- [23] V.A. Kalaev, Yu.E. Kalinin, A.V. Sitnikov and K.A. Sitnikov // *Perspective Materials* **6** (2005) 57, In Russian.